# Morphological and Mechanistic Aspects of Thiourea-Induced Acute Lung Injury and Tolerance in the Rat

Pellegrini, Giovanni ; Williams, Dominic Paul ; Amadio, Daniele ; Park, Brian Kevin ; Kipar, Anja

Abstract: Thiourea-based molecules cause pulmonary edema when administered to rats at relatively low doses. However, rats survive normally lethal doses after prior exposure to a lower, nonlethal dose; this phenomenon is known as tolerance. The present study investigated the morphological and functional aspects of acute lung injury (ALI) induced by methylphenylthiourea (MPTU) in the Wistar rat and the pulmonary response involved in prevention of the injury. We identified pulmonary endothelial cells as the main target of acute MPTU injury; they exhibited ultrastructural alterations that can result in increased vascular permeability. In tolerant rats, the lungs showed only transient endothelial changes, at 24-hour post dosing, and mild type II pneumocyte hyperplasia on day 7 post dosing. They exhibited glutathione levels similar to the controls and increased expression of flavin-containing monooxygenase 1 (FMO1), the enzyme responsible for bioactivation of small thioureas in the laboratory rat. Incubation of rat pulmonary microsomal preparations with MPTU inhibited FMO activity, indicating that tolerance is related to irreversible inhibition of FMOs. The rat model of thiourea-induced pulmonary toxicity and tolerance represents an interesting approach to investigate certain aspects of the pathogenesis of ALI and therapeutic approaches to lung diseases, such as acute respiratory distress syndrome.

DOI: https://doi.org/10.1177/0192623320941465

# Morphological and mechanistic aspects of thiourea-induced acute lung injury and tolerance in the rat

G. Pellegrini[1], D. Williams[2], D. Amadio[3], B.K.Park[4], and A. Kipar[1,5].

Affiliations:

1 Laboratory for Animal Model Pathology (LAMP), Institute of Veterinary Pathology, Vetsuisse Faculty, University of Zurich, Switzerland

2 Safety Platforms, Clinical Pharmacology and Safety Sciences, R&D, AstraZeneca, Cambridge CB4 0FZ, United Kingdom

3 Research and Early Development, Respiratory, Inflammation and Autoimmunity, BioPharmaceuticals R&D, AstraZeneca, Mölndal, Sweden

4 MRC Centre for Drug Safety Science, Department of Clinical and Molecular Pharmacology, Sherrington Building, Ashton Street, University of Liverpool, Liverpool, L69 3GE, UK.

5 Institute of Global Health, University of Liverpool, Liverpool Science Park IC2, 146 Brownlow Hill, Liverpool L3 5RF, UK

**Thiourea-induced tolerance in the lungs**

Pellegrini et al.

Corresponding author :

Giovanni Pellegrini, DVM, PhD, DiplECVP

Disclaimer

Dr. G. Pellegrini´s current address is: Clinical Pharmacology and Safety Sciences, R&D, AstraZeneca, Pepparedsleden 1, SE-431 83 Mölndal, Sweden, T: +46 (0)31 7762452 M: +46 (0) 72 2165780.
giovanni.pellegrini@astrazeneca.com

Dr. D. Amadio´s current address is: Pelago Bioscience AB, Banvaktsvägen 20, SE-171 48 Solna, Sweden T: +46 (0)76-941 01 87 M: +46 (0)36980108.
daniele.amadio@pelagobio.com

Keywords: acute lung injury; tolerance; thiourea; flavin containing monoxygenase; rat

Abbreviations: **ALI** Acute lung injury, **ANTU** Alpha-naphthylthiourea, **AQP-5** Aquaporin 5, **ARDS** acute respiratory distress syndrome, **CYP** cytochome P450, **FMO** Flavin-containing monooxygenase, **GSH** Gluthatione, **HE** Hematoxylin and eosin, **HD** High dose of MPTU (5 mg/kg), **LD** Low dose of MPTU (0.5 mg/kg),**MI** Methimazole, **MPTU** Methylphenylthiourea, **PCNA** Proliferating cell nuclear antigen, **PD** Post dosing, **S** Substrate, **SP-C** Surfactant protein C, **RT** Reverse transcription, **TEM** Transmission electron microscopy, **VO** velocity

## Abstract

Thiourea-based molecules cause pulmonary edema when administered to rats at relatively low doses. However, rats survive normally lethal doses after prior exposure to a lower, non-lethal dose; this phenomenon is known as tolerance. The present study investigated the morphological and functional aspects of acute lung injury (ALI) induced by methylphenylthiourea (MPTU) in the Wistar rat and the pulmonary response involved in prevention of the injury. We identified pulmonary endothelial cells as the main target of acute MPTU injury; they exhibited ultrastructural alterations that can result in increased vascular permeability. In tolerant rats the lungs showed only transient endothelial changes, at 24 hr post dosing, and mild type II pneumocyte hyperplasia on day 7 post dosing. They exhibited glutathione levels similar to the controls and increased expression of flavin-containing monooxygenase 1 (FMO1), the enzyme responsible for bioactivation of small thioureas in the laboratory rat. Incubation of rat pulmonary microsomal preparations with MPTU inhibited FMO activity, indicating that tolerance is related to irreversible inhibition of FMOs. The rat model of thiourea-induced pulmonary toxicity and tolerance represents an interesting approach to investigate certain aspects of the pathogenesis of ALI and therapeutic approaches to lung diseases, such as acute respiratory distress syndrome.

## Introduction

Acute single dose toxicity of thiourea in laboratory rodents and dogs is characterized by severe pulmonary edema.[1] Lung toxicity requires metabolic activation of thiourea[2], which is mainly carried out during phase I metabolism by the flavin containing monooxygenase enzymes (FMOs), of which thiourea is an excellent substrate.[3] FMO oxygenation of lipophilic compounds containing heterophilic atoms produces more polar, readily excreted metabolites with reduced pharmacological and toxicological properties. However, FMO-mediated S-oxygenation of small chemical groups such as sulphides and disulphides, thioethers, thiols and thioureas represents an exception to this rule and produces a sulphoxide, often through an intermediate sulphenic acid.[3] Sulphenic acids, which can be further oxidized to sulphinic and sulphonic acids, are extremely reactive electrophiles and are thought to react promptly with the parent drug or with nucleophiles such as glutathione (GSH) or other sulfhydryls to produce disulphides which disrupt the redox balance and induce oxidative stress, eventually resulting in irreversible modification of cellular proteins. [4,5]

The expression of the FMO genes varies considerably between different animal species[6], despite the relatively low number of genes (five functional members, FMO1 to FMO5) and allelic variants of this protein family. In the wild rat lung, FMO1 and FMO2 seem to be the only FMO members expressed at significant levels.[7] In laboratory rats, *FMO2* is mutated, encodes a truncated, catalytically inactive protein and does not contribute to the bioactivation of thiourea.[7]

Investigations into the toxic effects of thioureas were mainly conducted during the years surrounding World War II, when the risk of rat-borne epidemics was extraordinarily high; they led to the synthesis of alpha-naphthylthiourea (ANTU), an organosulphur compound containing the thiourea moiety and a naphthalene group.[8] ANTU was shown to cause severe respiratory distress in rats, resulting from pulmonary edema and pleural effusion, and subsequently became popular as an experimental model of lung edema and acute respiratory distress syndrome (ARDS).[9] ANTU proved to be an effective rodenticide but with major drawbacks[10], one of which was that rats that had survived a sublethal dose of the rodenticide were able to withstand subsequent lethal doses.[11] Several studies have attempted to explain the mechanism underlying tolerance to ANTU. [2, 12-13] Proliferation of epithelial cells in the lung was considered as a possible mechanism,[12] based on the observation that administration of keratinocyte growth factor to rats attenuated the pulmonary edema induced by the rodenticide.[14] However, the literature in this field has so far failed to illustrate in detail the pathological processes in the lung associated with tolerance and a definitive conclusion on the mechanism underlying the acquired tolerance to thiourea has not been drawn. Yet, the elucidation of the tolerance mechanism might bring new insights into potential therapeutic options for pulmonary conditions characterized by increased vascular permeability and oxidative stress, such as ARDS or adverse drug reactions (e.g. to bleomycin).[15]

The present study aimed to characterize the morphological changes and the mechanisms connected with the development of and adaptation to the acute pulmonary toxicity induced by a thiourea derivate (methylphenylthiourea,

henceforth named MPTU) in laboratory rats. Mechanistic knowledge in this field is particularly relevant since reactive oxygen scavengers, such as N-acetyl-cysteine or dimethylthiourea, are used as therapeutic adjuncts to prevent oxidant-mediated damage to the lung; these scavengers have been extensively studied in animal models of ARDS,[16] but their efficacy might vary based on the underlying pathogenesis. We hypothesized that the induction of tolerance after administration of a sublethal dose of MPTU could result from either increased clearance of edema fluid, increased levels of sulfhydryl-reducing agents, and/or altered expression/function of FMOs in the rat lungs and tried to address each of these postulations (Fig.1).

## Materials and Methods

### Test article

All experiments were conducted using a small thiourea derivate (MPTU, a phenylthiourea with a methyl substitution in position 6), provided by BASF Professional & Speciality Solutions, BASF plc, United Kingdom. MPTU was formulated on the same day and administered by oral intubation to rats, whilst control rats received only the vehicle (polyethylene glycol 200:triethanolamine).

### Experimental animal work

Male Wistar rats (6-7 weeks, 200-250 g) were obtained from Charles River Laboratories (Margate, UK). Upon arrival, all rats were maintained in environmentally controlled rooms with 12 hr dark-and-light cycles. They were caged in groups, with tap water and commercial rat food available *ad libitum*. All animal experiments were undertaken in accordance with criteria outlined in a license granted by the designated Scientific Procedures Establishment under the Animals (Scientific Procedures) Act 1986, which implements in the UK the EU Directive 86/609/EEC. The experimental protocols were approved by the University of Liverpool Animal Ethics Committee.

In order to identify the target organs and the toxicological changes induced by a lethal dose of MPTU, Wistar rats (n = 6) received po (gavage) 5 mg/kg of the test article, a dose that had been previously determined to exceed the $LD_{50}$ in acute toxicity studies conducted at our facility ($LD_{50}$ between 2 and 5 mg/kg; results not shown), and were euthanized at 6 hr post dosing (pd), after they had developed severe clinical signs. In a second pilot experiment, aimed to

study the development of tolerance, rats (n = 5) received a low oral dose (0.5 mg/kg) of MPTU, followed after 3 hr by a second, high dose (5 mg/kg). The tolerogenic dose was established based on a previously conducted experiment,[12] which achieved tolerance to a lethal dose of ANTU after the administration of a 10× lower tolerogenic dose. Clinical signs and mortality were monitored during the following 7 days (d). Based on the results of this experiment, a 14 d tolerance study was designed, as illustrated in Figure 2. Briefly, this study included four dose groups that received po the vehicle, the high dose (HD, 5 mg/kg) of MPTU, the low dose (LD, 0.5 mg/kg) of MPTU or the LD and HD combined. In the LD and LD+HD groups, 3 hr, 6 hr, 24 hr, 7 d and/or 14 d euthanasia endpoints were selected; all groups were comprised of 3 rats. In an attempt to determine whether animals previously dosed with the LD of MPTU exhibited prolonged decreased susceptibility to a lethal dose of the compound, two cohorts of three rats that had previously been administered the LD or the LD+HD received a further dose of 5 mg/kg in the morning of day 14 post initial treatment. All rats in these two additional cohorts were euthanized 6 hr after the challenge.

In all studies, clinical signs were recorded at 0, 0.5, 1, 2, 4, 6 and/or 8 hr pd and then twice daily, until the end of the experiments. Any animal that exhibited clinical signs such as tachypnea and dyspnea was constantly monitored and was culled according to the standard operating procedures in force before experiencing severe pain, distress or death.

**Post mortem examination**

Rats were euthanized with carbon dioxide, followed by exsanguination. A complete necropsy, including a thorough external and internal gross post mortem examination was performed on each rat. Any fluid that was present in the thoracic cavity was aspirated with a syringe, quantified and cytological specimens prepared, stained with May Grunwald Giemsa, and examined with a light microscope. A comprehensive histological examination including all organs and tissues was carried out in the first acute toxicity study (full pathological screening), whilst the histological analysis in all further experiments was limited to selected organs (brain, heart, lungs, liver, kidneys, thymus and spleen). The lungs were removed and, after ligation of the right hilus, fixed through gentle intratracheal instillation of 2 mL 4% buffered paraformaldehyde (pH 7.4). In the acute toxicity study, the lungs were not instilled with the fixative to allow assessment and quantification of intraalveolar fluid and cells. Light and transmission electron microscopy were performed on the left lobes and the right cranial lobes, respectively. The remaining right lobes (median, caudal and accessory lobes) were snap frozen in liquid nitrogen, stored at -80°C and used for the determination of GSH levels and for RT-qPCR. After 48 hr fixation, the left lobe was trimmed, processed and routinely paraffin wax embedded for histological examination. Serial sections (3-5 µm thick) were prepared and stained with hematoxylin and eosin (HE) and subjected to immunohistological staining. Microscopic findings in the HE-stained slides were classified with standard pathological nomenclature and severities of findings were graded on a scale of 1 to 5 as minimal (1), mild (2), moderate (3), marked (4), or severe (5). Grades of severity for microscopic

findings were subjective; minimal was the least extent discernible and severe was the greatest extent possible.[17]

Immunohistology was employed for the characterization of the cells populating the alveolar unit and to determine the presence of apoptotic and proliferating cells in the alveoli, detecting the following antigens: aquaporin 5 (AQP-5; type I pneumocytes), surfactant protein C (SP-C, type II pneumocytes), lysozyme (alveolar macrophages and type II pneumocytes)[18], von Willebrand factor (endothelial cells), cleaved caspase 3 (apoptotic cells) and proliferating cell nuclear antigen (PCNA, proliferating cells). See supplementary material at http://tpx.sagepub.com/supplemental for details regarding the immunohistological protocols and specifics of the antibodies used in this study. SP-C- and lysozyme-expressing cells were counted using ten 400 × magnification (i.e. high power) fields, avoiding areas at the periphery of the section or regions containing large bronchial and vascular structures. All positive and negative cells were counted in each field, and immunostained cells were quantified as a percentage of the total cells. For the quantification of PCNA-positive proliferating cells in the lung of rats from the tolerance study, twenty random fields were evaluated at the 400 × magnification and the proliferative index was expressed as the average number of PCNA-positive cells/field. Occasional positive cells other than alveolar lining cells, such as bronchial or bronchiolar epithelial cells, endothelial cells in arteries and veins as well as leukocytes were not included in the counts.

Transmission electron microscopy (TEM) was conducted on the lungs of selected animals (one rat/group, tolerance study). For this purpose, approximately 1 $mm^3$ samples of lung tissue from the cranial right lobe of all

animals were fixed in 2.5% glutaraldehyde in 0.1 M sodium cacodylate buffer, pH 7.4, for 24 hr and subsequently routinely embedded in epoxy resin. Semi-thin sections were prepared and stained with toluidine blue. From the semi-thin sections of one rat/group, areas of interest were chosen and ultrathin sections (60 nm) prepared, stained with Reynold's lead citrate and examined with a transmission electron microscope (Philips EM208S, Cambridge, UK).

**Determination of pulmonary glutathione (GSH) levels**

Total (oxidized and reduced) GSH amounts in the lungs were determined as described previously[19] from all rats in the tolerance study and normalized to the amount of proteins measured using the Lowry assay.[20] Briefly, approximately 200 mg of lung tissue (right middle and caudal lobes) was homogenized in 200 µL 6.5% (w/v) 5 sulfosalicylic acid and 800 µL GSH stock buffer (143 mM $NaH_2PO_4$ and 6.3 mM EDTA in distilled water, pH 7.4), using a manual glass homogenizer. The homogenates were incubated on ice for 10 min and then pelleted through centrifugation at 20,000 g for 5 min. The supernatant was collected and 1 mL of 1 M NaOH was added to each protein pellet and incubated at 60°C for 1 hr. The supernatant was used for the GSH assay which represented modified, previously published methods.[21,22] For the assay, 20 µL of supernatant diluted 1:10 and 1:20 or GSH standards (0-80 nM/mL) were added in duplicate to a 96-well microplate, followed by the addition of 20 µL GSH stock buffer to neutralize the pH. 200 µL of daily assay reagent (1 mM 5-5'-dithiobis[2-nitrobenzoic acid], 0.34 mM NADPH in GSH stock buffer) was added to each well. This was followed by an exact 5 min incubation at room temperature. The enzymatic reaction described above was

initiated by the addition of 50 µL GSH reductase (6.96 U/mL in GSH stock buffer, Sigma, Poole, UK). GSH formation was followed at 412 nm for 2.5 min in a MRX microplate reader (Dynotech Laboratories, Billinghurst, UK). All reagents were covered in aluminum foil to protect them from light.

**RT-qPCR for FMO1 and FMO2 mRNA quantification**

Reverse transcription (RT) was performed in all animals from the tolerance study on purified RNA extracted from lung tissue using TRIzol LS RNA reagent (Thermo Fisher Scientific, Paisley, UK), employing a TaqMan RNA reverse transcription kit (Thermo Fisher Scientific). Quantitative (q)PCR experiments were carried out following MIQE guidelines[23] and using an Opticon Monitor 2 real time PCR machine (MJ research, Biorad, Watford, UK). SYBR Green I-based Master Mix (SYBRGreen JumpStart Taq ReadyMix, Sigma) and pre-developed upstream and downstream primers specific to the FMO1 and FMO2 genes were used according to the manufacturer's protocol to quantitate the expression of genes in treated rats relative to the control animals. No-RT and no-template negative controls were included in each run. Results were evaluated using the Opticon Monitor software v.3.1.32 (MJ Research, Biorad) and normalized against the reference genes. See supplementary material at http://tpx.sagepub.com/supplemental for details on target (*FMO1* and *FMO2*) and reference (glyceraldehyde 3-phosphate dehydrogenase; *GAPDH*) genes, primer sequences and detailed PCR protocols.

**Enzyme assays**

FMO activity was estimated in rat lung microsomes, prepared from untreated rats as previously described,[24,25] using the methimazole (MI) assay.[26] Enzyme kinetics were determined using nine scalar concentrations (ranging from 5 μM to 1 mM) of the substrate and were calculated by plotting the reaction velocity (V0) as a function of the ratio between V0 and the substrate (S) concentration (Eadie–Hofstee diagram). The data sets were analyzed by GraphPad Prism version 6.00 for Windows (GraphPad Software, La Jolla, California, USA; www.graphpad.com, demo version) with a non-linear regression method that fits the Michaelis-Menten equation. The experiments were conducted in triplicate. Once the kinetic parameters were determined, FMO activity against MI over time (7 min) was measured, selecting a single substrate concentration (500 mM). The experiment was conducted in triplicate, at three different days. Negative controls, omitting the microsomal protein or MI, or composed exclusively of buffer, were included in each run. Enzyme inhibition was investigated, repeating the same experiment with the addition of the test article, MPTU (500 μM, resulting in a final concentration of approximately 75 μg).

**Note on data analysis**. A statistical analysis was not performed because of the small number of animals in each treatment group. Due to the low sample size, there was not enough data that could be summarized using summary statistics. Instead, univariate scatterplots were employed to present the results and compare magnitude of values.

~~**Statistical analysis**~~

~~Statistical analysis was conducted on cell counts for SP-C-, lysozyme- and PCNA-expressing cells, pulmonary GSH levels and relative pulmonary FMO1 and FMO2 mRNA levels, using the GraphPad Prism 8 software. Statistical analysis was performed by using the Kruskal Wallis non-parametric one-way ANOVA followed by Dunn´s multiple comparison test. All results were expressed as median ± standard deviation. Statistical significance was set at $p < 0.05$.~~

## Results

### Morphological features of acute pulmonary toxicity induced by MPTU

We carried out a single dose acute toxicity study in which rats received po a dose (5 mg/kg) of MPTU known to be lethal based on the results of a pilot acute toxicity study. Most animals were not eating or drinking from 3 hr pd onwards, and all rats were electively euthanized starting at 6 hr pd, after they had developed progressively severe clinical signs suggestive of impaired general health and respiratory distress, such as tachypnea, dyspnea, hunched posture and decreased motor activity. At necropsy, all treated rats exhibited pleural effusion (hydrothorax) with 3 to 6 ml of clear, transparent fluid in the thoracic cavity (Figure 3) the cytological examination of which showed low cellularity, with occasional individualized non-reactive mesothelial cells within a moderately proteinaceous background, indicating the fluid was a transudate. The main histological changes were found in the lungs of the treated animals (Figure 4) and consisted of severe multifocal alveolar edema, characterized by the presence of a moderate to high amount of eosinophilic, homogenous or faintly granular material in the alveolar lumen (Figure 4B). Similar proteinaceous material was observed in the interstitium surrounding bronchi and blood vessels (interstitial edema; Figure 4D). A ~~mild~~ small increase in the number of alveolar macrophages (lysozyme-positive and SP-C-negative) was observed within the alveolar lumen. The alveolar architecture appeared otherwise unaltered, with a continuous lining by AQP-5-positive type I pneumocytes and von Willebrand factor-positive endothelial cells (data not shown). However, several treated rats exhibited scattered apoptotic alveolar lining cells, confirmed by their expression of cleaved caspase 3 (Figure 4F).

The ultrastructural examination (Figure 5) identified these apoptotic cells as endothelial cells. In the lungs of the rat euthanized at 6 hr pd, the general ultrastructural architecture of the alveolar unit was preserved. However, subendothelial blebs were detected within the alveolar capillaries (Figure 5B), these resulted from the separation of the endothelial cell from the underlying basal lamina and ranged from 100 nm to 1 μm in diameter. The blebs usually contained material with an electron density similar to that found in the capillary lumen, it was therefore interpreted as plasma. In addition, the endothelial lining appeared multifocally discontinuous (Figure 5C), as indicated by an irregular endothelial cell surface and occasional gap formation adjacent to intercellular junctions. In proximity to the gaps within or between endothelial cells, the alveolar lumen contained proteinaceous material with an electron density similar to that of plasma (alveolar edema; Figure 5D). Endothelial cells often appeared swollen and showed rarefaction or swelling of organelles and caveolae. Rarely, they also exhibited signs of irreversible injury, i.e. apoptosis (nuclear condensation and fragmentation; see also above, Figure 5C).

**Morphological features of the pulmonary adaptive response induced by MPTU**

The administration of non-lethal doses of the thiourea-based rodenticide ANTU to rats results in the development of tolerance to normally lethal doses.[12] In order to investigate whether this was also the case for MPTU, a pilot study was undertaken in which rats received a low dose (0.5 mg/kg) of MPTU, followed only 3 hr later by the normally lethal dose. Rats did not succumb to the high dose and only showed piloerection and mild tachypnea that both

resolved within less than 48 hr, suggesting they had developed the expected tolerance. In the 14 d tolerance study, which comprised rats that received the low dose alone (0.5 mg/kg; LD) and rats administered the low dose, followed 3 hr later by the high dose (5 mg/kg; LD+HD), no relevant clinical signs or gross findings were observed in any animal. Histological changes in the lungs were similar in the two groups, as summarized in Table 1. While there was no evidence of alveolar and interstitial edema in LD rats euthanized at early time points (3, 6 and 24 hr), this was observed with mild severity in one LD+HD animal euthanized at 24 hr pd (3 and 6 hr time points were not included in the study design for LD+HD animals).Most rats in both groups exhibited minimal to mild type II pneumocyte (SP-C-positive) hyperplasia, which was observed at 24 hr pd, was most obvious at day 7 pd and was no longer present on day 14 (Figures 6 and 7). PCNA immunohistology indicated an increase in proliferating alveolar lining epithelial cells consistent with type II pneumocytes at day 7. For comparison, only rare or no PCNA-positive alveolar cells were seen in control animals and in treated rats euthanized at early time points (LD rats: 3, 6 and 24 hr; LD+HD rats: 24 hr ) and at 14 d (Figure 6 and 7). In addition, an increase in alveolar macrophages was observed in LD animals at the 6 and 24 hr time points and LD+HD rats at 24 hr, similar in its extent to the increase seen in the high dose rats euthanized at 6 hr; a less pronounced increase, was observed at 7 and 14 d pd (Figure 7).

Ultrastructural evaluation of the lungs at early time points (3, 6 and 24 hr pd) after the administration of tolerogenic doses of MPTU revealed endothelial blebs identical to those described in rats that had received the high dose (Figure 8A), however, these were far less frequently encountered and were

not detected at later time points (7 and 14 d pd). Other ultrastructural changes observed after administration of the high dose alone, such as gap formation and apoptosis of capillary endothelial cells, were not detected in the tolerant rats. Instead, undifferentiated pneumocytes (so called "intermediate" cells)[27] were found with increased frequency in rats euthanized at 24 hr and 7 d pd (Figure 8B, C). These cells exhibited large, oval to elongated, sometimes slightly indented, electron lucent nuclei with finely stippled chromatin and small amounts of cytoplasm devoid of lamellar bodies or other organelles, except for the endoplasmic reticulum.[28,29] Such undifferentiated pneumocytes were very rare in the control animals, in tolerant rats at earlier time points, or in rats that had received the high dose only, where up to 3 cells/ultrathin section (approximately 200 $mm^2$) were found. In the tolerant rats they were detected in almost every alveolar unit at the 24 hr and 7 d time points.

All rats from the two additional cohorts that were euthanized 6 hr after challenge on day 14 with the high dose showed moderate dyspnea for up to 2 hr; this correlated with a moderate to severe hydrothorax (3-5 mL). Histologically, pulmonary alveolar and interstitial edema was seen in all rats (data not shown), with similar incidence and severity as in rats receiving the high dose alone. These data suggest that tolerance was considerably attenuated 2 weeks after initial administration of a tolerogenic dose.

**Effects of methylphenylthiourea on pulmonary GSH content and FMO expression**

GSH levels in rats that had received the high dose, including those that were challenged on day 14 after initial tolerance induction, were reduced to

approximately 10% of those measured in the controls (Figure 9A). In rats administered MPTU at tolerogenic doses they were comparable or only moderately lower than in controls, suggesting that pulmonary antioxidant defenses are not increased in the tolerant lungs.

We explored the potential role of FMO1 in the development of thiourea-related toxicity and tolerance using RT-qPCR and also measured the FMO2 transcripts, since although the enzyme is inactive and not present in the lungs of laboratory rats, its mRNA levels are not influenced by the FMO2 genotype and the absence of protein in the tissue is due to altered translation or protein instability rather than transcription impairment.[7] In tolerant rats euthanized at 24 h pd and later, regardless of the dose administered, FMO1 mRNA levels were ~~significantly ($p < 0.05$)~~ increased (Figure 9B), showing a 3-fold elevation at day 7 pd. Similarly, FMO2 mRNA levels were ~~significantly ($p < 0.01$)~~ higher in all treated animals than in controls, including those euthanized at the earliest time points (3 and 6 hr pd, Figure 9C~~B~~).

**Analysis of enzyme inhibition**

The Eadie-Hofstee graphical representation of methimazole (MI) S-oxidase activity catalyzed by FMOs in rat lung microsomal pools (Figure 10A) consisted of a straight line, suggesting that oxygenation of MI in these preparations was predominantly a monophasic reaction, carried out by FMO1.[7] Catalytic activities of pulmonary FMO were investigated in rat pulmonary microsomes monitoring the change in absorbance at 412 nm for 7 min after the addition of a single dose (500 mM) of MI to the incubations. This experiment was repeated with 500 mM of MPTU added to the incubations and comparing the curves

obtained to those generated by incubations containing only MI or buffer. Obvious non competitive inhibition was noted, as indicated by the striking reduction in the absorbance change following the addition of the test article to the microsomal preparations (Figure 10B).

## Discussion

Acute pulmonary toxicity caused by molecules containing a thiourea moiety, including the thiourea-based compound ANTU, is characterized by acute pulmonary edema resulting from increased vascular permeability,[30] similarly to what we observed with our test article, methylphenylthiourea (MPTU). Our results confirm that paracellular gap formation in pulmonary capillary endothelial cells represents the most likely morphological equivalent of the increased permeability. Structural damage to endothelial cells was mild in our studies and likely contributed only to a minor extent. The pulmonary architecture was well preserved and there was no loss of integrity of the alveolar epithelial cell lining, indicating that the epithelial compartment does not represent a (primary) target of thiourea toxicity.

We then assessed the development of tolerance in the lung of rats administered sublethal doses of MPTU and investigated the pulmonary changes that contribute to the decreased susceptibility of tolerant rats to high, normally lethal doses of this thiourea-derived molecule. Barton et al. achieved complete protection from a lethal dose of ANTU (70 mg/kg) in rats administered a low, single dose (5 mg/kg) 24 hr before challenge with the high dose.[12] In order to set up a tolerogenic regimen for our test article, a tolerogenic:lethal dose ratio similar to that reported by Barton et al. was used and the rats were initially given a dose (0.5 mg/kg) of MPTU which was 10 × lower than the $LD_{50}$ (5 mg/kg). In none of the previous studies rats were challenged with the lethal dose before 24 hr after tolerance induction;[11-13] surprisingly, we found that protection against the high dose challenge was already effective as early as 3 hr after the administration of the tolerogenic

dose. This indicates that tachyphylaxis induced by thiourea-based molecules may represent an extremely effective protective mechanism that develops more rapidly than previously thought.[12] As expected, tolerant animals only showed very mild clinical signs that were paralleled by the ultrastructural evidence of occasional endothelial bleb formation, irregular endothelial lining and rare paracellular gap formation. These findings were similar to but considerably less severe than those observed in the animals that had received only the lethal dose. This suggests that while the pathological processes induced by MPTU are not affected during the tolerogenic response, their degree is reduced, producing milder effects on the air blood barrier. Similar to other investigations,[12,13] we also observed severe clinical signs and pulmonary edema in previously tolerant rats challenged after 14 d with the lethal dose of MPTU, suggesting that the protection conferred by a tolerogenic dose is phasing out within 2 weeks.

Both histology and immunohistology concurred to ~~demonstrate~~ identify a trend towards ~~a substantial~~ increase in the number of macrophages and type II pneumocytes in the lungs of tolerant rats when compared to controls and high dose rats. The differing kinetic behavior of these cell populations is interesting: the early reaction (at 3, 6 and 24 hr pd) was represented by an influx of alveolar macrophages into the alveolar lumen, whilst type II pneumocytes ~~began~~ appeared to increase in number at 24 hr pd and reached maximum levels on day 7. On day 14, the number of both alveolar macrophages and type II pneumocytes ~~had~~ seemed to have almost returned to the levels observed in the controls. The rise in macrophages and type II pneumocytes appeared to be time- rather than dose-dependent, as the increases were of a similar degree

both in rats given the low dose only or the combined doses. The ultrastructural examination of type II epithelial cells allowed an important distinction: whilst the lungs of the tolerant rats at day 7 were predominantly populated by type II epithelial cells exhibiting numerous large lamellar bodies, the alveolar septa of rats euthanized at 6 and 24 hr pd exhibited numerous undifferentiated epithelial cells, with intermediate features between type I and type II pneumocytes. The transient appearance of an intermediate epithelial cell phenotype is consistent with differentiation of type II pneumocytes into type I pneumocytes following alveolar damage, as previously described.[27-29, 31] This concept explains the low number of PCNA-positive cells observed at the 24 hr endpoint, suggesting that differentiation of type II pneumocytes into type I cells started shortly after MPTU-induced injury of the alveolar unit. The proliferation of type II cells observed at the later stage, evidenced by the increase in PCNA-positive cells at 7 d pd, likely represents a second phase.

A considerable amount of literature has been published looking into the defense mechanisms which are supposed to play a role in the adaptive response of the lungs following exposure to sublethal doses of thiourea-based molecules.[2,12-13] Several reports suggested that alveolar epithelial hyperplasia protects rodents from oxidative injury induced by hyperoxia,[32] bleomycin,[33,34] and hydrogen peroxide,[35] as increased cellularity in the alveoli~~us~~ may strengthen the alveolar barrier, enhance the clearance of alveolar fluid[36,37] and/or influence the levels of inflammatory mediators and oxygen radical scavengers in the lung.[14] Our work showed that protection from a lethal dose of MPTU is achieved after only 3 hr from the administration of a tolerogenic dose, when there is no morphologic evidence of an increased number of cells

in the lungs. This suggests that clearance of alveolar fluid by increased numbers of alveolar macrophages and type II pneumocytes in the lungs of tolerant rats may well contribute to the amelioration of the respiratory distress observed after the first few hours, but it is unlikely the primary mechanism associated with the development of tolerance.

With this in mind, we speculated that the adaptive response could have resulted from an enhancement of the antioxidant defense system. It is well known that the lungs are able to upregulate their protective antioxidant scavenging systems when exposed to mild oxidative injury, as occurs for instance in the lungs of chronic smokers.[38] This is usually achieved by increasing the expression of antioxidant enzymes such as superoxide dismutase or, more frequently, glutathione peroxidase, which leads to larger amounts of GSH available to counteract the oxidative insult. This mechanism is unlikely to have an important role in the adaptive process that occurs in MPTU-tolerant lungs, as we observed GSH levels that ~~were~~ appeared to be at all time points similar to or lower than those found in the control rats.

Several drugs are able to modulate the levels of FMO expression in different tissues, either directly or through stimulation of an inflammatory response and production of inflammatory mediators, such as nitric oxide.[39] Recently, upregulation of FMO3 has been described as a possible factor contributing to the development of resistance to hepatotoxicity caused by paracetamol in mice.[40] We thought this could also be the case for MPTU and hypothesized that tolerance to thioureas might depend on the downregulation of FMO expression in the lungs and consequently decreased levels of the enzymes that are able to catalyze the oxygenation of these molecules to the reactive

intermediates responsible for the oxidative injury. We found ~~significantly~~ higher FMO1 and FMO2 mRNA levels in tolerant rats compared to controls, indicating that the decreased susceptibility to pulmonary oxidative injury in tolerant rats does not rely on the downregulation of the enzymes responsible for the metabolism of thiourea-based molecules.[3]

It remained to be explored whether tolerance could be consistent with a mechanism of noncompetitive inhibition of FMOs, according to which the metabolic products of MPTU would have an inhibitory effect on the enzyme, even directly or through the formation of protein adducts or complexes with FMOs, leading to its inactivation. Indeed, addition of the test article to lung microsomal preparations prevented FMO-mediated oxygenation of MI, indicating inhibition of FMO activity. Although time-dependent inhibition has not been previously described for FMOs, it is known to alter the potency and influence the activity of cytochrome P450 (CYP).[41] It is characterized by irreversible or quasi-irreversible inactivation of the enzyme, which causes lack of function of CYP until new protein is synthesized, typically after several days.[41] Therefore, the transient (less than 14 days) duration of MPTU-induced tolerance, coupled with increased synthesis of FMO1 and FMO2 mRNA, ~~is~~ appears to be consistent with a time-dependent inhibition of FMOs which is then progressively lost with synthesis of new protein.[41] The outcome of these experiments provides preliminary *in vitro* evidence of irreversible FMO inhibition by MPTU and might lead to a possible mechanistic explanation for the acquired tolerance. It needs confirmation by *ex vivo* approaches, i.e. the testing of FMO activity in microsomes obtained directly from rats exposed to MPTU and euthanized at different time points. Also, we used a single

tolerogenic dose in both our *in vitro* and *in vivo* studies, while it would be interesting to investigate the effectiveness of MPTU in inducing tolerance, and the associated morphological changes resulting from a range of tolerogenic doses in order to confirm the mode of action of MPTU. The role of FMO inhibition in the development of tolerance to MPTU (and possibly to other oxidative scavengers) could also be addressed by using different synthetic FMO inhibitors in both *in vitro* and *in vivo* experiments. Furthermore, the small group size (n=3) and the inclusion of only one control group at 24 hr represents ~~a~~ limitations of the tolerance~~bility~~ study. Group numbers were determined based on the outcomes of pilot toxicity studies, which showed limited variability of the evaluated parameters within a dose group; they were deemed sufficient for this exploratory research work and are in line with the 3Rs principles. However, caution must be applied when generalizing the findings beyond the context of this study.

The model of ALI caused by phenylthiourea shares numerous features with ARDS, a severe human pulmonary condition characterized by diffuse acute oxidative damage of the alveolar unit, which is not completely understood to date and difficult to treat.[42] All available animal models of ALI aim to reproduce the mechanisms and consequences observed in humans by inducing significant damage to the alveolar epithelium, which is followed by a reparative process.[42] The main limitation of experimental models of ALI is that none fully recapitulate the features of lung injury in humans. Thioureas may represent an interesting and unique model of ALI, where the primary injury affects the endothelial cells rather than the epithelial compartment, similar to oleic acid and endotoxin, which are commonly used as ALI models that target mainly the

capillary endothelium.[42] In addition, further understanding of the mechanisms involved in the development of tolerance to thiourea-induced ALI might be helpful to develop therapeutic strategies aimed at reducing the severity of lung injury. For example, it would be interesting to test whether cell proliferation induced by small doses of MPTU can protect the lungs from ALI caused by different noxious agents such as toxic gases, hyperoxia, endotoxins and viral infection, and more recently, e-cigarette vaping[43] and whether this could be of clinical relevance. Future studies should assess the significance of the pulmonary responses to this type of injury and determine whether they still represent a reparative process or are instead an adaptive reaction, aimed to confer protection from further injury. With this in mind, the investigation of these protective mechanisms may bring new insight into the therapeutic approach to ALI and ARDS in humans.

## Figure legend

Figure 1. Potential mechanisms underlying tolerance to MPTU addressed in the present study include increased clearance of alveolar fluid, increased antioxidant defenses, and reduced FMO activity. The molecule depicted in the drawing is phenylthiourea. Phenylthiourea (1) is transformed into a phenylthiourea reactive intermediate, i.e. a sulfenic acid (2) with consumption of GSH. The S-oxidation of the molecule is carried out by FMOs. Redrawn from Smith and Crespi (2002).[44]

Figure 2. Schematic timeline representation of the 14 day tolerance experiment. n: number of rats euthanized at each time point. Group sizes for each time point are n = 3. MPTU: methylphenylthiourea.

Figure 3. Macroscopic features of MPTU-induced acute lung toxicity. Severe hydrothorax (*) in a rat administered a high dose (5 mg/kg) of MPTU and euthanized 6 hr post dosing.

Figure 4. Microscopic features of MPTU-induced acute lung toxicity. (A-D) Severe alveolar and interstitial edema, represented by proteinaceous fluid filling the alveolar lumen (B, *) and the perivascular space (D, double-headed arrow) of the same rat as in figure 3 (5 mg/kg) of MPTU). Figures A and C show normal alveoli and interstitial space in a control rat lung for comparison. Hematoxylin and eosin stain. Bars: 20 µm. (E-F) Apoptotic alveolar lining cells are observed in the lungs of a treated rat (F, arrow) compared to a control lung (E) where no apoptotic cells are detected. Cleaved caspase 3 immunohistochemistry. Bars: 20 µm.

Figure 5. Ultrastructural features of MPTU-induced acute lung toxicity. (A) Normal alveolar unit in a control rat. Type I pneumocytes are separated from the underlying capillary endothelial cells by a fused continuous basal lamina (arrowhead). (B-D) Treated rat administered with a high dose (5 mg/kg) of MPTU and euthanized 6 hr

post dosing. (B) Subendothelial blebs (arrow) in the alveolar unit. (C) Inter-endothelial cell gap (open arrowhead) in the vicinity of the cellular junction, alongside a subendothelial bleb (arrow). Apoptotic endothelial cells (solid arrowhead) are observed infrequently. (D) Proteinaceous fluid in the air-blood barrier (arrows) and the alveolar lumen (*). Bars: 2 µm.

Table 1. Summary of the key histological findings in MPTU-induced pulmonary toxicity and tolerance. Results are expressed as number of animals showing the histological finding/number of animals per group. The average severity of each finding [in brackets] was calculated by summing the severity grades and dividing the total by the number of animals affected by that finding.

Figure 6. Microscopic features of MPTU-induced tolerance in the lungs. (A-D) Compared to the control lungs (A), type II pneumocyte hyperplasia is evident at 24 hr post dosing (pd) (B), increases in severity at day 7 pd and is no longer present on day 14 pd (D). In each figure, the right panel shows the SP-C immunohistology for type II pneumocytes (arrows). (E-F) Compared to the control lungs (E), in which no PCNA-positive alveolar cells are noted, staining for PCNA reveals an increase in proliferating alveolar lining epithelial cells (arrows) consistent with type II pneumocytes at day 7 pd (F). Bars: 10 µm.

Figure 7. Immunohistological features (cell count) of MPTU-induced tolerance in the lungs. (A) Percentages of total cells expressing SP-C (type II pneumocytes). An increase in type II pneumocytes is observed on day 7 pd. (B) Number of cells in the alveoli~~us~~ expressing PCNA. An increase is evident on day 7 pd. (C) Percentages of cells within the alveolar lumen expressing lysozyme (alveolar macrophages). An increase is observed at the 6 hr and 24 hr pd. Data are presented as mean percentage of positive cells/total cells/field/animal (SP-C, lysozyme) or number of positive cells/field/animal (PCNA). ~~The height of the bars and the number within each bar~~

represent the median. HD: high dose of MPTU (5 mg/kg). LD: low dose of MPTU (0.5 mg/kg).

Figure 8. Ultrastructural features of MPTU-induced tolerance in the lungs. (A) Subendothelial bleb (arrowhead) in the alveolar unit of a tolerant rat (0.5 mg/kg + 5 mg/kg of MPTU, 24 hr pd). (B) An immature pneumocyte (arrowhead) in the alveolius of a tolerant rat (0.5 mg/kg of MPTU, 24 hr pd). (C) Numerous immature pneumocytes (arrowheads) in the alveolar unit of a tolerant rat (0.5 mg/kg of MPTU) euthanized 24 hr pd, together with type II pneumocytes (arrows). (D) Numerous type II pneumocytes (arrows) in the lungs of a tolerant rat (0.5 mg/kg of MPTU) at 7 d pd. Bars: 2 µm.

Figure 9. GSH levels and FMO expression in the lungs of rats administered the high dose (HD, 5 mg/kg) of MPTU, the low dose alone (LD, 0.5 mg/kg) or the LD, followed 3 hr later by the HD (LD + HD). (A) An increase in GSH levels is seen at the 6 hr pd time points, also in the rat cohorts challenged with the HD on day 14 and euthanized 6 hr later (bold outlines). (B) qPCR analysis showing significantly higher levels of relative expression (fold change) of FMO1 and FMO2 in the lungs of rats following exposure to high and low doses of MPTU. The height of the bars and the number within each bar represent the median. * $p < 0.05$ ** $p < 0.01$ (Kruskal Wallis non parametric ANOVA)

Figure 10. Catalytic activities of FMO in rat pulmonary microsomes and enzyme inhibition using MPTU. (A) Enzyme kinetics of the sulphoxygenation of methimazole (MI) deduced from the Michaelis Menten equation. Reaction velocity is plotted in an Eadie-Hofstee diagram against the ratio between velocity and substrate concentration and is represented by a monophasic reaction. Data points for each replicate are

represented. Dashed lines indicate the 95% confidence intervals for the regression line. Vmax: maximum velocity of the reaction. Km: Michaelis-Menten constant. (b) MI (500 mM) oxygenation rates over time (7 min) and inhibitory activity of MPTU on the sulphoxygenation of MI. Difference in absorbance (ΔOD) is plotted against time. ~~Data are presented as median ± standard deviation for n=9 (three different measurements obtained from three independent experiments).~~

# References

1 Ziegler-Skylakakis, K et al. Thiourea. Concise International Chemical Assessment Document. No. 49. World Health Organization, Geneva, 2003; pp. 1-37. https://apps.who.int/iris/handle/10665/42606. Accessed January 03, 2019.

2 Boyd, MR and Neal, RA. Studies on the mechanism of toxicity and of development of tolerance to the pulmonary toxin, alpha-naphthylthiourea (ANTU). Drug Metab Dispos. 1976; 4(4): 314-322.

3 Krueger SK and Williams DE. Mammalian flavin-containing monooxygenases: structure/function, genetic polymorphisms and role in drug metabolism. Pharmacol Ther. 2005; 106: 357–387.

4 Henderson MC, Siddens LK, Krueger SK, et al. Flavin-containing monooxygenase S-oxygenation of a series of thioureas and thiones. Toxicol Appl Pharmacol. 2014; 278(2): 91-99.

5 Mansuy, D and Dansette, PM. Sulfenic acids as reactive intermediates in xenobiotic metabolism. Arch Biochem Biophys. 2011; 507(1): 174-185.

6 Cashman, JR and Motika, MS. Monoamine oxidases and flavin-containing monooxygenases. In: Mcqueen, CA. Comprehensive toxicology. 2nd ed. Elsevier, Oxford; 2010: 95-103.

7 Hugonnard, M, Benoit, E, Longin-Sauvageon, C and Lattard, V. Identification and characterization of the FMO2 gene in Rattus norvegicus: a good model to study metabolic and toxicological consequences of the FMO2 polymorphism. Pharmacogenetics. 2004; 14(10): 647-655.

8 Richter, CP. The development and use of alpha-naphthyl thiourea (ANTU) as a rat poison. J Am Med Assoc. 1945; 129: 927-931.

9 Yilmaz Sipahi, E. Experimental models of acute respiratory distress syndrome. J Transl Int Med. 2015; 2(4): 154-159.

10 Keiner, C. Wartime rat control, rodent ecology, and the rise and fall of chemical rodenticides. Endeavour. 2005; 29(3): 119-125.

11 Dieke, SH and Richter, CP. Age and species variation in the acute toxicity of alphanaphthyl thiourea. Proc Soc Exp Biol Med. 1946; 62: 22-25.

12 Barton, CC, Bucci, TJ, Lomax, LG, Warbritton, AG and Mehendale, HM. Stimulated pulmonary cell hyperplasia underlies resistance to alpha-naphthylthiourea. Toxicology. 2000; 143(2): 167-181.

13 Van Den Brenk, HA, Kelly, H and Stone, MG. Innate and drug-induced resistance to acute lung damage caused in rats by alpha-naphthyl thiourea (ANTU) and related compounds. Br J Exp Pathol. 1976; 57(6): 621-636.

14 Mason, CM, Guery, BP, Summer, WR and Nelson, S. Keratinocyte growth factor attenuates lung leak induced by alpha-naphthylthiourea in rats. Crit Care Med; 1996: 24(6): 925-931.

15 Aeffner F, Bolon B, Davis IC. Mouse Models of Acute Respiratory Distress Syndrome: A Review of Analytical Approaches, Pathologic Features, and Common Measurements. Toxicol Pathol. 2015; 43(8): 1074-1092.

16 Gonzalez, PK, Zhuang, J, Doctrow, SR et al. Role of oxidant stress in the adult respiratory distress syndrome: evaluation of a novel antioxidant strategy in a porcine model of endotoxin-induced acute lung injury. Shock. 1996; 6 Suppl(1): 23-26.

17 Shackelford C, Long G, Wolf J, Okerberg C, Herbert R. Qualitative and quantitative analysis of nonneoplastic lesions in toxicology studies. Toxicol Pathol. 2002; 30(1): 93–96.

18 Singh, G, Katyal, SL, Brown, WE, Collins, DL and Mason, RJ. Pulmonary lysozyme-a secretory protein of type II pneumocytes in the rat. Am Rev Respir Dis. 1988; 138(5): 1261-1267.

19 Williams DP, Antoine DJ, Butler PJ, et al. The metabolism and toxicity of furosemide in the Wistar rat and CD-1 mouse: a chemical and biochemical definition of the toxicophore. J. Pharmacol. Exp. Ther. 2007(3); 322: 1208-1220.

20 Lowry, OH, Rosebrough, NJ, Farr, A.L. and Randall, RJ. Protein measurement with the Folin phenol reagent. J Biol Chem. 1951; 193: 265-275.

21 Owens, CW and Belcher, RV. A Colorimetric Micro-Method for the Determination of Glutathione. Biochem J. 1965; 94: 705-711.

22 Vandeputte, C, Guizon, I, Genestie-Denis, I, Vannier, B and Lorenzon, G. A microtiter plate assay for total glutathione and glutathione disulfide contents in cultured/isolated cells: performance study of a new miniaturized protocol. Cell Biol Toxicol. 1994; 10(5-6): 415-421.

23 Bustin, SA, Benes V, Garson JA, et al. The MIQE guidelines: minimum information for publication of quantitative real-time PCR experiments. Clin Chem. 2009; 55(4): 611-622.

24 Gill, HJ, Tingle, MD and Park, BK. N-Hydroxylation of dapsone by multiple enzymes of cytochome P450: implications for inhibition of haemotoxicity. Br J Clin Pharmacol. 1995; 40(6): 531-538.

25 Philpot, RM, Arinc, E and Fouts, JR. Reconstitution of the rabbit pulmonary microsomal mixed-function oxidase system from solubilized components. Drug Metab Dispos. 1975; 3(2): 118-126.

26 Dixit, A and Roche, TE. Spectrophotometric assay of the flavin-containing monooxygenase and changes in its activity in female mouse liver with nutritional and diurnal conditions. Arch Biochem Biophys. 1984; 233(1): 50-63.

27 Uhal BD. Cell cycle kinetics in the alveolar epithelium. Am J Physiol. 1997; 272(6 Pt1): L1031–1045

28 Adamson, IY and Bowden, DH. The type 2 cell as progenitor of alveolar epithelial regeneration. A cytodynamic study in mice after exposure to oxygen. Lab Invest. 1974; 30(1): 35-42.

29 Evans, MJ, Cabral, LJ, Stephens, RJ and Freeman, G. Transformation of alveolar type 2 cells to type 1 cells following exposure to NO2. Exp Mol Pathol. 1975; 22(1): 142-150.

30 Meyrick, B, Miller, J and Reid, L. Pulmonary oedema induced by ANTU, or by high or low oxygen concentrations in rat-an electron microscopic study. Br J Exp Pathol. 1972; 53(4): 347-358.

31 Fehrenbach H. Alveolar epithelial type II cell: defender of the alveolus revisited. Respir. Res. 2001; 2(1): 33–46

32 Panos, RJ, Bak, PM, Simonet, WS, Rubin, JS and Smith, LJ. Intratracheal instillation of keratinocyte growth factor decreases hyperoxia-induced mortality in rats. J Clin Invest. 1995; 96(4): 2026-2033.

33 Deterding, RR, Havill, AM, Yano, T, et al. Prevention of bleomycin-induced lung injury in rats by keratinocyte growth factor. Proc Assoc Am Physicians. 1997; 109(3): 254-268.

34 Sugahara, K, Iyama, K, Kuroda, MJ and Sano, K. Double intratracheal instillation of keratinocyte growth factor prevents bleomycin-induced lung fibrosis in rats. J Pathol. 1998; 186(1): 90-98.

35 Chapman, KE, Waters, CM and Miller, WM. Continuous exposure of airway epithelial cells to hydrogen peroxide: protection by KGF. J Cell Physiol. 2002; 192(1): 71-80.

36 Guery, BP, Mason, CM, Dobard EP, et al. Keratinocyte growth factor increases transalveolar sodium reabsorption in normal and injured rat lungs. Am J Respir Crit Care Med. 1997; 155(5): 1777-1784.

37 Sznajder, JI, Ridge, KM, Yeates, DB, Ilekis, J and Olivera, W. Epidermal growth factor increases lung liquid clearance in rat lungs. J Appl Physiol. 1998; 85(3): 1004-1010.

38 Comhair, SA and Erzurum, SC. Antioxidant responses to oxidant-mediated lung diseases. Am J Physiol Lung Cell Mol Physiol. 2002; 283(2): L246-255.

39 Park CS, Baek HM, Chung WG, Lee KH, Ryu SD, and Cha YN. Suppression of flavin-containing monooxygenase by overproduced nitric oxide in rat liver. Mol Pharmacol. 1999; 56(3): 507–514

40 O'Connor, MA, Koza-Taylor, P, Campion, SN, et al. Analysis of changes in hepatic gene expression in a murine model of tolerance to acetaminophen hepatotoxicity (autoprotection). Toxicol Appl Pharm. 2013; 274 (1): 156-67.

41 Riley, RJ, Grime, K and Weaver, R. Time-dependent CYP inhibition. Expert Opin Drug Metab Toxicol. 2007; 3(1): 51-66.

42 Matute-Bello, G, Frevert, CW and Martin, TR. Animal models of acute lung injury. Am J Physiol Lung Cell Mol Physiol. 2008; 295(3): L379-399.

43 Butt, JM, Smith ML, Tazelaar HD, et al. Pathology of Vaping-Associated Lung Injury. New England Journal of Medicine, 2019; 381(18): 1780-1781.

44 Smith, PB and Crespi, C. Thiourea toxicity in mouse C3H/10T1/2 cells expressing human flavin-dependent monooxygenase 3. Biochem Pharm. 2002; 63(11): 1941-1948.

| MPTU Dose (mg/kg) | Time of death pd | Histological findings | | | |
|---|---|---|---|---|---|
| | | Alveolar and interstitial edema | Increase in alveolar macrophages | Type 2 pneumocyte hyperplasia | Alveolar cell apoptosis |
| 0 | 24 hr | 0/3 | 0/3 | 0/3 | 0/3 |
| 5 | 6 hr | 3/3 [2.6] | 3/3 [2] | 0/3 | 2/3 [1.5] |
| 0.5 | 3 hr | 0/3 | 3/3 [1.6] | 0/3 | 0/3 |
| | 6 hr | 0/3 | 3/3 [2] | 0/3 | 0/3 |
| | 24 hr | 0/3 | 3/3 [2] | 2/3 [1] | 0/3 |
| | 7 d | 0/3 | 1/3 [1] | 3/3 [1.3] | 0/3 |
| | 14 d | 0/3 | 1/3 [1] | 0/3 | 0/3 |
| 0.5 + 5 (3 hr later) | 24 hr | 1/3 [2] | 3/3 [3] | 2/3 [1.3] | 1/3 [2] |
| | 7 d | 0/3 | 2/3 [1.5] | 3/3 [2] | 0/3 |
| | 14 d | 0/3 | 2/3 [1] | 1/3 [1] | 0/3 |

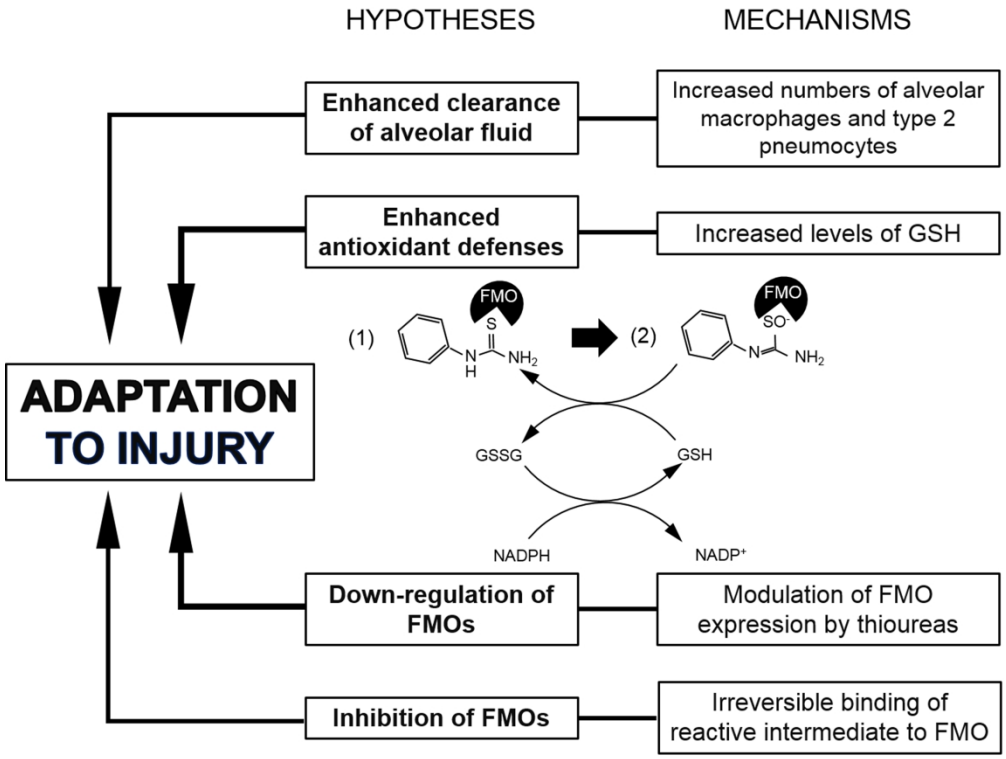


Potential mechanisms underlying tolerance to MPTU addressed in the present study include increased clearance of alveolar fluid, increased antioxidant defences, and reduced FMO activity. The molecule depicted in the drawing is phenylthiourea. Phenylthiourea (1) is transformed into a phenylthiourea reactive intermediate, i.e. a sulfenic acid (2) with consumption of GSH. The S-oxidation of the molecule is carried out by FMOs. Redrawn from Smith and Crespi (2002).44

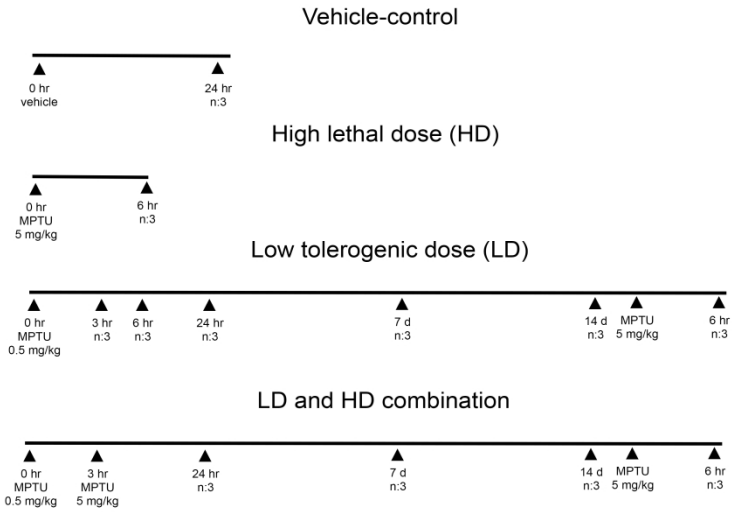


Schematic timeline representation of the 14 day tolerance experiment. n: number of rats euthanized at each time point. Group sizes for each time point are n = 3. MPTU: methylphenylthiourea.

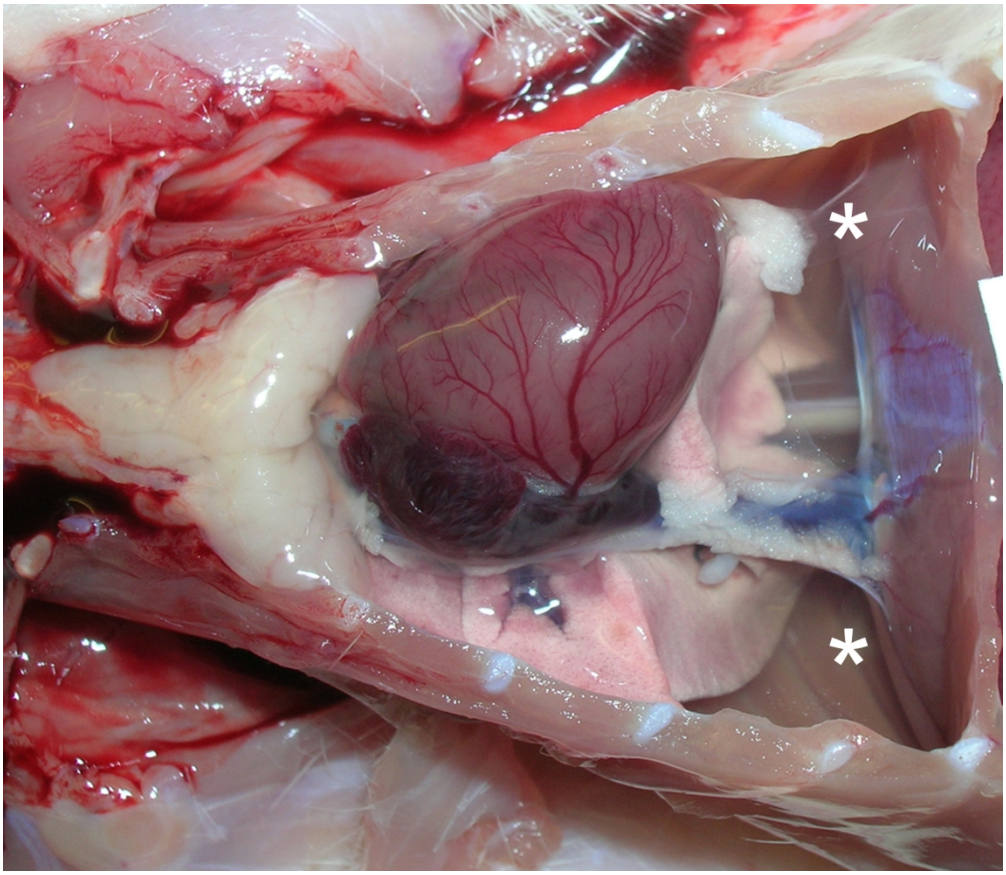


Macroscopic features of MPTU-induced acute lung toxicity. Severe hydrothorax (*) in a rat administered a high dose (5 mg/kg) of MPTU and euthanized 6 hr post dosing.

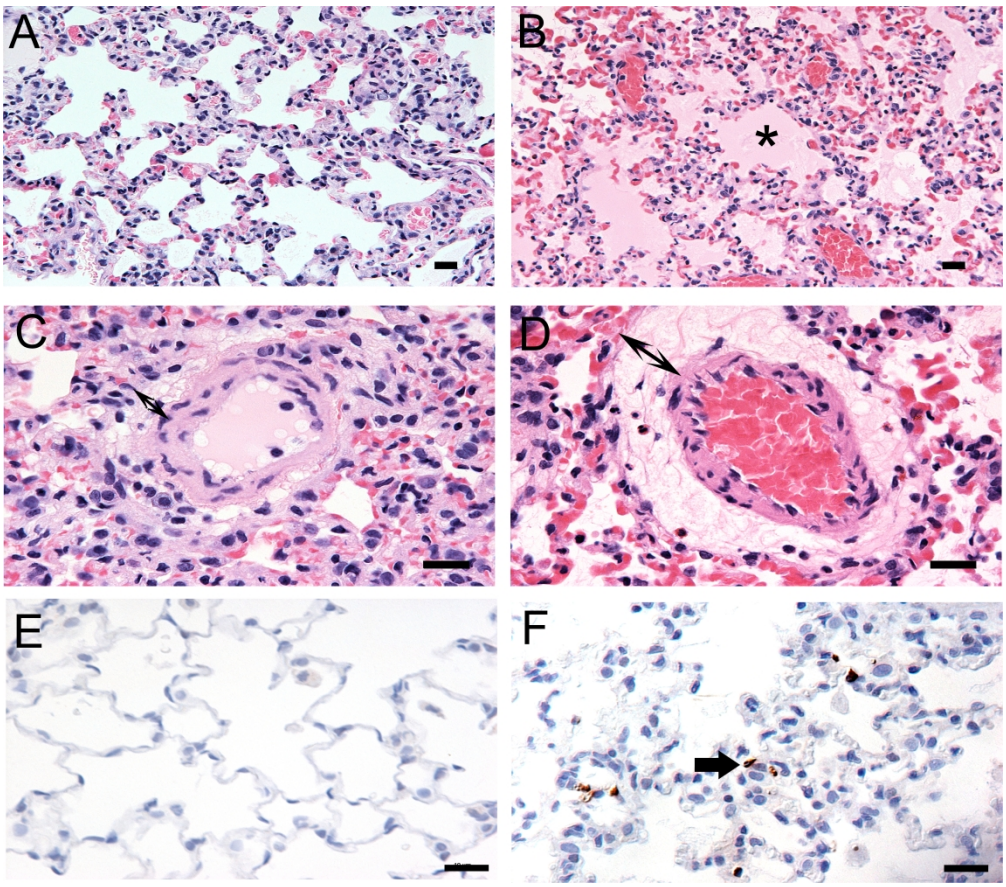


Microscopic features of MPTU-induced acute lung toxicity. (A-D) Severe alveolar and interstitial edema, represented by proteinaceous fluid filling the alveolar lumen (B, *) and the perivascular space (D, double-headed arrow) of the same rat as in figure 3 (5 mg/kg) of MPTU). Figures A and C show normal alveoli and interstitial space in a control rat lung for comparison. Hematoxylin and eosin stain. Bars: 20 µm. (E-F) Apoptotic alveolar lining cells are observed in the lungs of a treated rat (F, arrow) compared to a control lung (E) where no apoptotic cells are detected. Cleaved caspase 3 immunohistochemistry. Bars: 20 µm.

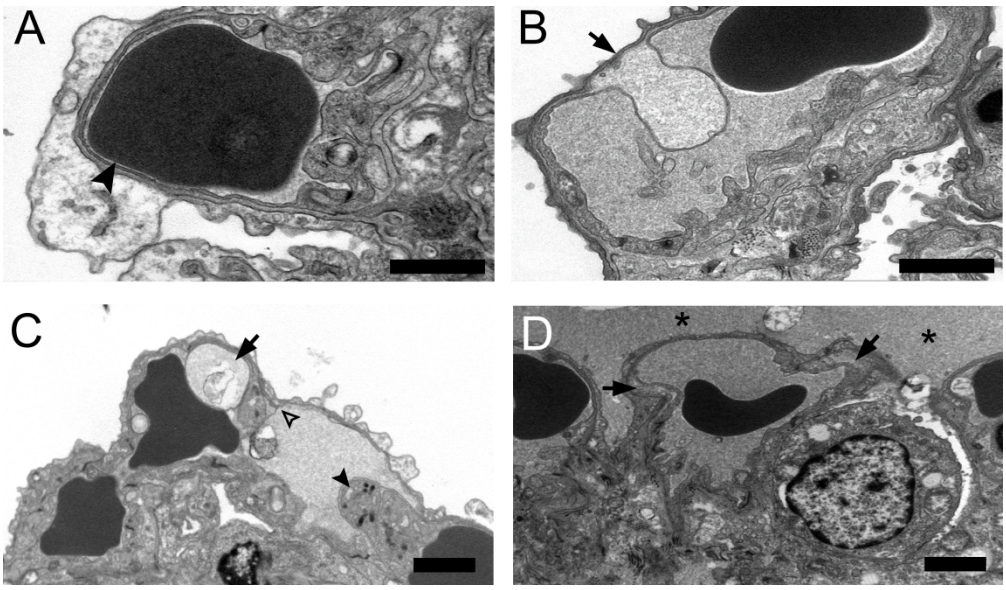


Ultrastructural features of MPTU-induced acute lung toxicity. (A) Normal alveolar unit in a control rat. Type I pneumocytes are separated from the underlying capillary endothelial cells by a fused continuous basal lamina (arrowhead). (B-D) Treated rat administered with a high dose (5 mg/kg) of MPTU and euthanized 6 hr post dosing. (B) Subendothelial blebs (arrow) in the alveolar unit. (C) Inter-endothelial cell gap (open arrowhead) in the vicinity of the cellular junction, alongside a subendothelial bleb (arrow). Apoptotic endothelial cells (solid arrowhead) are observed infrequently. (D) Proteinaceous fluid in the air-blood barrier (arrows) and the alveolar lumen (*). Bars: 2 μm.

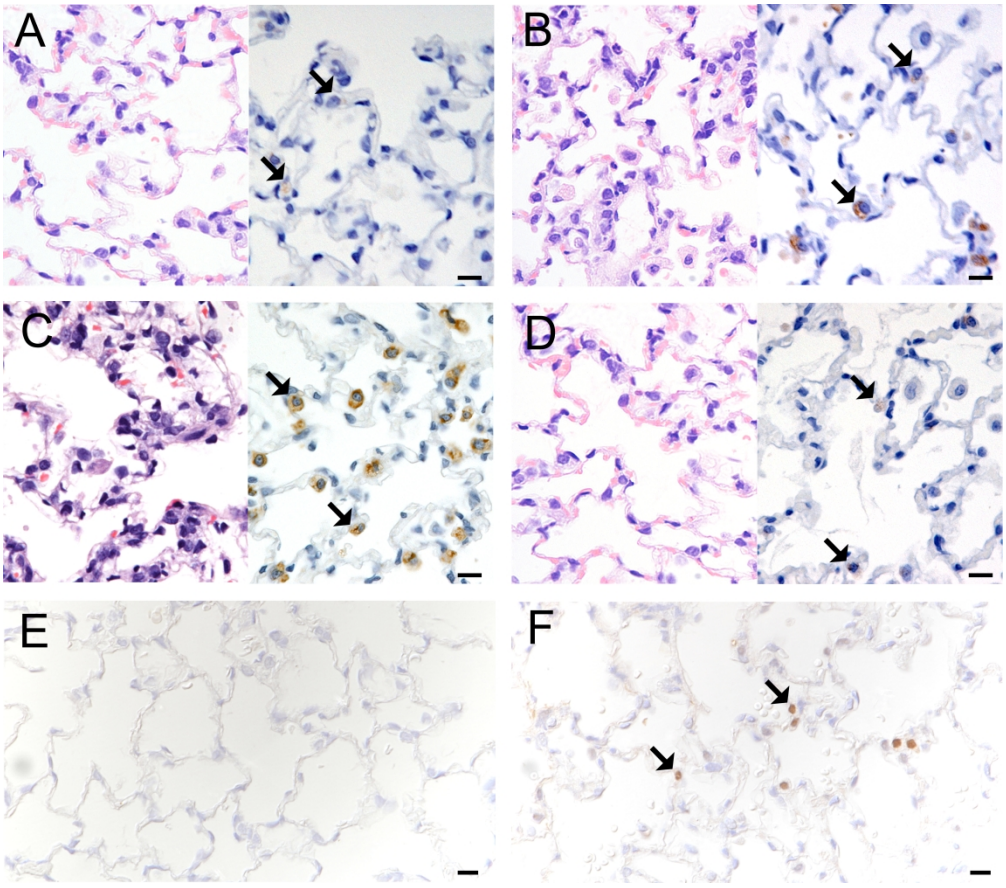


Microscopic features of MPTU-induced tolerance in the lungs. (A-D) Compared to the control lungs (A), type II pneumocyte hyperplasia is evident at 24 hr post dosing (pd) (B), increases in severity at day 7 pd and is no longer present on day 14 pd (D). In each figure, the right panel shows the SP-C immunohistology for type II pneumocytes (arrows). (E-F) Compared to the control lungs (E), in which no PCNA-positive alveolar cells are noted, staining for PCNA reveals an increase in proliferating alveolar lining epithelial cells (arrows) consistent with type II pneumocytes at day 7 pd (F). Bars: 10 μm.

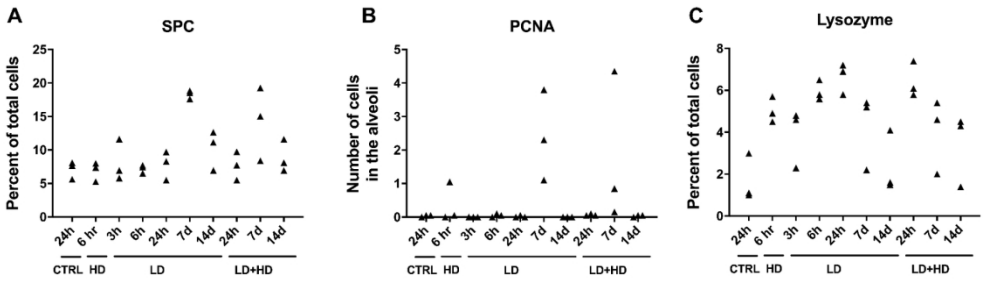


Immunohistological features (cell count) of MPTU-induced tolerance in the lungs. (A) Percentages of total cells expressing SP-C (type II pneumocytes). An increase in type II pneumocytes is observed on day 7 pd. (B) Number of cells in the alveolius expressing PCNA. An increase is evident on day 7 pd. (C) Percentages of cells within the alveolar lumen expressing lysozyme (alveolar macrophages). An increase is observed at the 6 hr and 24 hr pd. Data are presented as mean percentage of positive cells/total cells/field/animal (SP-C, lysozyme) or number of positive cells/field/animal (PCNA).HD: high dose of MPTU (5 mg/kg). LD: low dose of MPTU (0.5 mg/kg).

159x47mm (300 x 300 DPI)

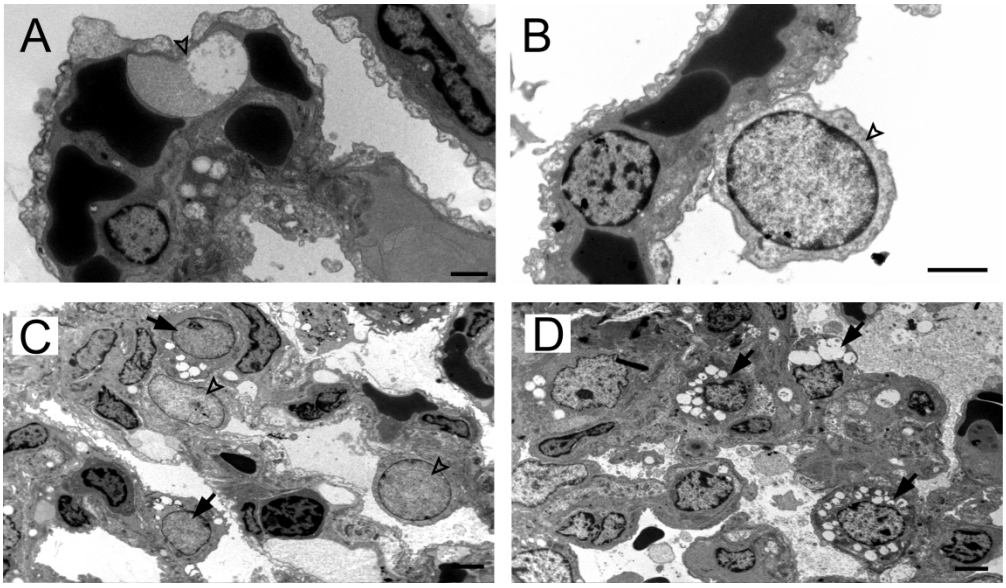


Ultrastructural features of MPTU-induced tolerance in the lungs. (A) Subendothelial bleb (arrowhead) in the alveolar unit of a tolerant rat (0.5 mg/kg + 5 mg/kg of MPTU, 24 hr pd). (B) An immature pneumocyte (arrowhead) in the alveolus of a tolerant rat (0.5 mg/kg of MPTU, 24 hr pd). (C) Numerous immature pneumocytes (arrowheads) in the alveolar unit of a tolerant rat (0.5 mg/kg of MPTU) euthanized 24 hr pd, together with type II pneumocytes (arrows). (D) Numerous type II pneumocytes (arrows) in the lungs of a tolerant rat (0.5 mg/kg of MPTU) at 7 d pd. Bars: 2 μm.

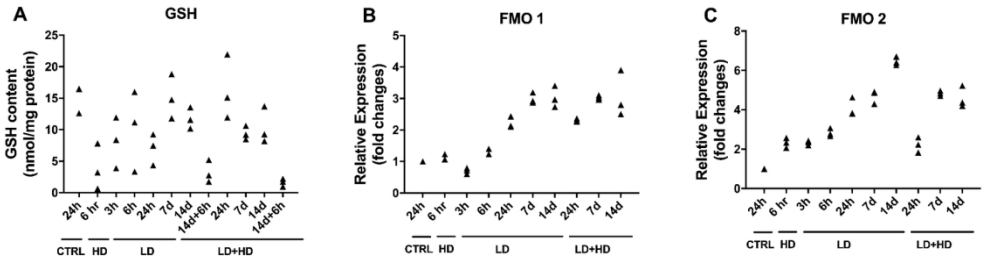


GSH levels and FMO expression in the lungs of rats administered the high dose (HD, 5 mg/kg) of MPTU, the low dose alone (LD, 0.5 mg/kg) or the LD, followed 3 hr later by the HD (LD + HD). (A) An increase in GSH levels is seen at the 6 hr pd time points, also in the rat cohorts challenged with the HD on day 14 and euthanized 6 hr later. (B) qPCR analysis showing higher levels of relative expression (fold change) of FMO1 and FMO2 in the lungs of rats following exposure to high and low doses of MPTU.

159x44mm (300 x 300 DPI)

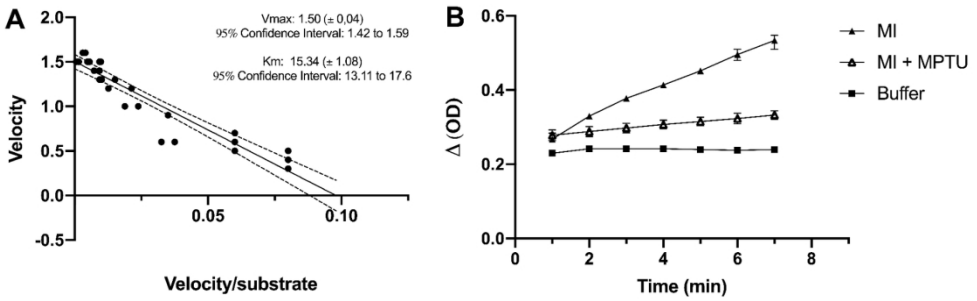


Catalytic activities of FMO in rat pulmonary microsomes and enzyme inhibition using MPTU. (A) Enzyme kinetics of the sulphoxygenation of methimazole (MI) deduced from the Michaelis Menten equation. Reaction velocity is plotted in an Eadie-Hofstee diagram against the ratio between velocity and substrate concentration and is represented by a monophasic reaction. Data points for each replicate are represented. Dashed lines indicate the 95% confidence intervals for the regression line. Vmax: maximum velocity of the reaction. Km: Michaelis-Menten constant. (b) MI (500 mM) oxygenation rates over time (7 min) and inhibitory activity of MPTU on the sulphoxygenation of MI. Difference in absorbance (ΔOD) is plotted against time.

160x53mm (300 x 300 DPI)

# Morphological and mechanistic aspects of thiourea-induced acute lung injury and tolerance in the rat

G. Pellegrini[1], D. Williams[2], S. Hughes[3], R. Sharples[3], B.K.Park[4], and A. Kipar[1,5].

## Immunohistology

Summary of the antibodies and other reagents used for immunohistology.

| Antibody | Antigen retrieval | Block | Primary antibody dilution | Secondary antibody dilution | Detection |
|---|---|---|---|---|---|
| **Caspase 3 (Cell Signaling 9664)** | Citrate pH 6.0 | 20% ss in TBST | 1:50 in 20% ss in TBST | Swine anti Rabbit IgG 1:100 in 20% ss in TBST (Dako Z0196) | PAP Rabbit 1:20 in 20% ss in TBST (Covance SMI) |
| **PCNA (Dako M0879)** | Citrate pH 4.0 | 10% rat serum in TBST | 1:100 in TBST | Rat anti Mouse 1:100 in TBST (Jackson Immuno Research 415-005-166) | PAP Mouse 1:500 in TBST (Jackson Immuno Research) |
| **Aquaporin 5 (Abcam ab78486)** | None | 20% ss in TBST | 1:100 in 20% ss in TBST | Swine anti Rabbit 1:100 in 20% ss in TBST | PAP Rabbit 1:20 in 20% ss in TBST |
| **Factor VIII (Dako A0082)** | Protease | ss:TBST 1:2 | 1:1000 in 20% ss in TBST | | |
| **SP-C (Santa Cruz sc-13979)** | None | 20% ss in TBST | 1:50 in TBST | | |
| **Lysozyme (Dako A0099)** | Protease | ss:TBST 1:2 | 1:1000 in 20% ss in TBST | | |

ss = swine serum. TBST = 1× TBS Buffer + 0.05% Tween 20

## RT-qPCR for FMO1 and FMO2 mRNA quantification

Primers used in qPCR.

| Primer name | NCBI reference sequence | Primer Sequence 5' → 3' | Melting t°C | GC% | Product length (bp) |
|---|---|---|---|---|---|
| **FMO1 forward** | NM_012792.1 | GATGACCTCCTGACCTCG | 60.9 | 61.1 | 142 |
| **FMO1 reverse** | | CTCCTTCCCACTTTCCTG | 59.8 | 55.5 | |
| **FMO2 forward** | NM_144737.2 | TCAAAGACCCTAAACTGGCTGTG | 60.7 | 47.8 | 103 |
| **FMO2 reverse** | | ATGGCATTCCTGGCTCCTTC | 67.5 | 55 | |
| **GAPDH1 forward** | NM_017008 | CCCATCACCATCTTCCAGGAG | 67.9 | 57.1 | 285 |
| **GAPDH1 reverse** | | GTTGTCATGGATGACCTTGGC | 66.6 | 52.3 | |
| **GAPDH2 forward** | | TGGAGTCTACTGGCGTCTT | 60.1 | 52.6 | 138 |
| **GAPDH2 reverse** | | TGTCATATTTCTCGTGGTTCA | 60.6 | 38.0 | |

Thermal cycling conditions of target and reference gene qPCR amplification.

| Step | t C° | Time | Number of cycles |
|---|---|---|---|
| Initial denaturation | 94 | 10 min | 1 |
| Denaturation | 94 | 30 sec | 35 |
| Annealing | 60 (FMO1 and GAPDH2)<br>63.5 (FMO2 and GAPDH1) | 30 sec | |
| Extension | 72 | 30 sec | |
| Primer dimer melt off | 75 | 1 sec | |
| Plate reading | - | - | |
| Final extension | 72 | 5 min | 1 |
| Melting temperature | 65-95 (increment 0.2/sec) | | 1 |
| Soak | 4 | indefinite | 1 |